Adsorption and Catalytic Activation of CO_2 on a $Au_{19}Pt$ Subnanometer Cluster in Aqueous Environment

Krishnakanta Mondal,*,† Megha,‡,¶ Arup Banerjee,‡,¶ and Alessandro Fortunelli§

†*Department of Physics, Central University of Punjab, Bathinda, India-151401*

‡*Human Resources Development Section, Raja Ramanna Centre for Advanced Technology, Indore 452013, India*

¶*Homi Bhabha National Institute, Training School Complex, Anushaktinagar, Mumbai 400094, India*

§*CNR-ICCOM, Consiglio Nazionale delle Ricerche, ThC2-Lab, Pisa 56124, Italy*

E-mail: krishnakanta1987@gmail.com

Abstract

Electrocatalytic reduction of CO_2 molecule has attracted attention of researchers as this technique offers alternative promising scheme for CO_2 utilization. The choice of appropriate materials for catalyst to accomplish the reduction reaction plays a crucial role. In this paper we employ ab-initio density functional theory based method to access the efficacy of subnanometer gold based $Au_{19}Pt$ cluster towards the electrocatalytic reduction of CO_2 molecule. We find, first, that $Au_{19}Pt$ gets spontaneously negatively charged in water even at zero bias, and, second, importantly, that the water environment selectively promotes the adsorption and activation of CO_2 on the $Au_{19}Pt$ anion. On the negatively charged $Au_{19}Pt$ the activation of CO_2 occurs through charge transfer from the cluster to the molecule via hybridization between the p-orbital of the

O-atoms of CO_2 and the partially filled d-orbitals of Pt-atom of the cluster. These results suggest $Au_{19}Pt$ as a promising subnanometer electrocatalyt for the reduction of CO_2.

Introduction

Currently, the whole world is facing an acute environmental threat of global warming due to the increasing level of CO_2 concentration in the atmosphere.[1] The present concentration of CO_2 in the atmosphere is above 400 ppm and, this is 100 ppm higher than the one reported in the year 1950. The increase in the level of CO_2 leads to the rise of the average temperature of the atmosphere.[1] The recycling of CO_2 gas present in the environment to useful chemical would be a practical way to tackle this problem.[2] In this direction extensive research work is being carried out by various groups throughout the world.[3–8] The hydrogenation of CO_2 towards the chemicals like ethanol, methanol, DME, which can be mixed with gasoline to fuel motor vehicles, is found to be a successful route to recycle CO_2. However, the conversion of the highly stable CO_2 molecule into these chemicals through hydrogenation is very challenging. In the last few decades researchers have extensively investigated the hydrogenation of CO_2 towards methanol which has the potential to dominate the source of future energy.[9–11] It is well-known that $Cu/ZnO/Al_2O_3$ act as a catalyst for industrial production of methanol from gas mixture of CO_2, CO and H_2.[5,12–14] Recently, it is reported that the Ce_2O_3/Cu systems exhibit better catalytic activity than ZnO/Cu systems for the hydrogenation of CO_2 to fuel.[15] These thermo-catalysts require very high temperature (400-500 K) and pressure (40-100 bar) for the conversion of CO_2 to fuel. Moreover, the reactor setup for the thermo-catalysis reaction for CO_2 to fuel is complicated and also expensive. On the other hand, the electrocatalytic reactor setup is relatively simpler as well as cheaper. Due to the simple implementation the electrocatalytic conversion of CO_2 into fuel is drawing attention of the researchers. Recently, it has been reported[16] that the electrocatalytic conversion of CO_2 to Formic acid is more favorable than to methanol on Pd-Polyaniline complex, which is in line

with the experimental observation.[17] Moreover, it is reported that copper is a very important heterogeneous catalyst which exhibits promising catalytic activity to produce valuable hydrocarbons and alcohol like ethylene and ethanol from electrochemical reduction of CO_2.[18,19] However, CO_2 to fuel conversion efficiency of the existing catalysts are very low. Therefore, researchers are looking for more efficient catalyst for the conversion of CO_2 to fuel. Recently, the adsorption and activation of CO_2 on gold based clusters and nano-particles have been extensively reported in the literature.[20–24] It is observed that the gold clusters doped with different transition metals like Cu, Pd, Sn, Pd, Ru, Ag etc. exhibit enhanced catalytic activity towards the conversion of CO_2 to fuel.[20–24] However, to the best of our knowledge there is no report on the catalytic activity of the gold-platinum bimetallic clusters towards the adsorption and activation of CO_2. Note that in the family of transition metals, Pt emerges as a unique element for its application as a catalyst for various industrially and environmentally important reactions including the hydrogenation of CO_2 to fuel.[25–27] Therefore, it will be interesting to investigate the catalytic activity of the gold-platinum bimetallic clusters for the adsorption and activation of CO_2 molecule.

Very recently, the electrocatalytic activity of gold and platinum clusters and nanoparticles for different reactions namely, hydrogen evolution reaction, oxygen reduction reaction, CO_2 reduction and catalytic oxidation reactions have been extensively reported in the literature.[21–23,28,29] Moreover, it is observed that the mixture of the gold and platinum exhibits more efficient thermo- and electro-catlytic activity as compared to their individual systems.[29] Furthermore, in a recent experiment it is reported that the electrocatalytic activity of Au_{25} cluster for the formic acid oxidation gets enhanced due to the doping with a single Pt atom.[29] These encouraging results motivate us to investigate the effect of a single Pt doping on CO_2 adsorption and activation behaviour of a gold cluster.

In the family of gold clusters Au_{20} possesses a very special position due to its highly symmetric tetrahedral (T_d) structure which is very stable in nature. Due to this stability Au_{20} generally does not take part in the catalytic reactions. However, it is reported that with

the help of suitable doping elements we can enhance the catalytic activity this cluster.[30,31] In particular, it is found that Pt is a suitable doping element due to its comparable size with Au atom and also it is capable of activating Au_{20} for various reactions namely, CO oxidation, H_2O_2 oxidation etc. In the quest of catalytic behaviour of Au_{20} cluster for the adsorption and activation of CO_2, in the present work we investigate the interaction of CO_2 molecule with $Au_{19}Pt$ clusters. Moreover, to understand the electrocatalytic activity of these clusters towards adsorption and activation of CO_2 we carry out the investigation in the presence of water environment. Interestingly, we find that $Au_{19}Pt$ clusters are negatively charged even at zero potential when we use water as electrolyte and Pt-cathode as a reference electrode. Therefore, we carry out the investigation on the adsorption and activation of CO_2 on the anion of $Au_{19}Pt$ cluster in water environment. Moreover, to identify the effect of water environment, we compare these results of the activation and adsorption of CO_2 with the corresponding gas phase results.

In the next section we discuss the computational methods used for the present work. The results are discussed in the section 3 and the work is summarised in the last section.

Computational Details

All the calculations in the present paper have been carried out by employing Amsterdam Density Functional (ADF2018) program package.[32,33] In order to account for the relativistic effect which is quite significant for Au atom, we perform the calculations using the scalar relativistic method based on zeroth-order regular approximation (ZORA).[34] All the doped structures are optimized at the GGA level with Perdew-Burke-Ernzerhof (PBE) exchange-correlation (XC) functional.[35] Note that this functional gives quite accurate results for structural and electronic properties of gold clusters and hence it is widely used to investigate pure as well as doped gold clusters.[36–39] We use triple-ζ Slater type orbital (STO) added with two polarization functions (TZ2P in ADF basis library) for the valence electrons. The frozen

cores considered for various atoms are 1s-4f for Au and Pt atoms and 1s for C and O atoms. The geometries are optimized using quasi-Newton method and the Hessian is updated in the optimization process by employing Broyden-Fletcher-Goldfarb-Shanno (BFGS)[40–43] method until the convergence criteria of 10^{-4} a.u. for cartesian gradient and 10^{-6} a.u. for energy are met. The stability of the clusters is checked with the vibrational frequency data. Absence of imaginary value of vibrational frequency indicates a stable structure. All the geometric structures presented in the current work are generated by using the VESTA[44] software. For calculations of CO_2 adsorption on the clusters we use RPBE[35,45] XC functional with van-der Waals (vdW). It is reported that this blend method can obtain more accurate adsorption energies.[46] To incorporate van-der Waals interaction we use Grimme's dispersion correction of 2010 as implemented in ADF.[47] Note that RPBE with Grimme's dispersion correction of 2010 (DFT-D3) is found to provide accurate structure of liquid water.[48] For completeness the CO_2 adsorption data calculated using PBE + vdW are given in the supplementary.

To understand the electrocatalytic behavior of the negative ions of $Au_{19}Pt$ cluster we investigate the interaction of CO_2 with $Au_{19}Pt$ clusters in water environment. The effect of water environment on the adsorption and activation of CO_2 has been captured using COSMO implicit solvent model as implemented in ADF. In this model we use the values of the dielectric constant and the radius of the (rigid sphere) solvent molecule as 78.39 and 1.39 Å, respectively. Using Pt as electrode in water we find that $Au_{19}Pt$ clusters are negatively charged even at zero bias. Details of the charging process has been discussed in the next section.

Results and discussion

Before going to study the structural and CO_2 adsorption behaviour of $Au_{19}Pt^-$ clusters we first discuss the process in which $Au_{19}Pt$ clusters become negatively charged. Through out this paper we denote the doped tetrahedral $Au_{19}Pt^-$ clusters by Td-X, where Td stands

for tetrahedral geometry and X (X = S (surface), E (edge), and V (vertex)) refers to the location of the dopant atom Pt.

Charging Process of $Au_{19}Pt$ Clusters

In this subsection we discuss a charging process for $Au_{19}Pt$ clusters. For this purpose we calculate the electron affinity (EA) of the clusters. In the gas phase EA of Td-E, Td-S and Td-V clusters are 5.37, 5.27 and 5.72 eV respectively. Solvation energies (E_s) of the charged species in water can be estimated via an implicit-solvent polarizable continuum model using the Born formula as,.[49]

$$E_s = -\frac{1}{2}\frac{q^2}{R} \tag{1}$$

where q is the charge and R is the radius of the cluster. In our case, R is approximately 15.28 a.u for all the three clusters and q = 1. Therefore, E_s is calculated as 0.89 eV for our clusters. As a results EA for Td-E, Td-S and Td-V clusters in water are 6.26, 6.16 and 6.61 eV, respectively.

Now, to estimate the charge transfer from the electrode to the clusters we need to calculate the energy of an electron. We consider Pt as electrode and water as electrolyte. The work function (WF) of Pt electrode at zero charge is 6.167 eV which changes in water environment to 5.167 eV.[50,51] The energy require to charge a cluster in the presence of Pt electrode can be estimated using the following equation:

$$E_p = WF_{Pt(bias=0.0V)} - EA \tag{2}$$

where, $WF_{Pt(bias=0.0V)}$ is the WF of Pt at zero bias. The values of E_p for Td-E, Td-S and Td-V are calculated as -1.09, -1.00 and -1.44 eV, respectively. These results show that the clusters are spontaneously negatively charged even at zero potential. Here, we wish to note that the work function of the commonly used carbon electrode[52] is around 3.4 eV (for

graphite) which is less than that of the Pt electrode. This indicates that $Au_{19}Pt$ clusters will also be negatively charged when we use graphitic carbon as electrode. In the following subsections we discuss the interaction of CO_2 with these negatively charged clusters.

Interaction of CO_2 with $Au_{19}Pt^-$ in the Gas Phase

Before discussing the results for the adsorption CO_2 molecule on $Au_{19}Pt^-$ clusters, we briefly describe the structural properties of the $Au_{19}Pt^-$ clusters. The detailed analysis on the structural properties of the neutral $Au_{19}Pt$ clusters can be found in our earlier work.[30] In the present work all the anionic structures of the $Au_{19}Pt$ cluster are optimized using density functional theory at GGA level with PBE exchange-correlation functional as implemented in ADF. The optimized structures of $Au_{19}Pt^-$ clusters generated from the tetrahedral structure of Au_{20} are shown in Figure 1. In this figure the relative energies of the corresponding $Au_{19}Pt^-$ clusters are given in the parenthesis. We find that the structures of $Au_{19}Pt^-$ clusters remain pyramidal as observed for the neutral clusters which are already discussed in our earlier work.[30] For the anions of $Au_{19}Pt$ cluster, it is observed that Td-E is the most stable structure whereas, Td-S and Td-V are slightly ($\sim$0.1 eV) less stable than Td-E. Such a very small energy differences among the isomers of $Au_{19}Pt^-$ cluster indicate that all the isomers can co-exist in the experiment. These results of the anions of $Au_{19}Pt$ are in contrast to the corresponding neutral systems, where Td-S was found to be the most stable one and Td-V was the least stable isomer of $Au_{19}Pt$.[30] This indicates that the charging of $Au_{19}Pt$ clusters alters the stability of these clusters.

Now, to investigate the interaction of CO_2 with $Au_{19}Pt^-$ clusters we place CO_2 at different non-equivalent positions of the clusters. The structures of all the $Au_{19}Pt$-CO_2 complexes are then optimized using RPBE XC functional along with van-der Waals correction taken into account of Grimme's D3 dispersion scheme. Following the notations adopted for the parent structures, we denote the various tetrahedral isomers of cluster-CO_2 complex by the symbol Td-X-Y, where Y refers to the site of CO_2 adsorption like S, E and V in the tetrahedral

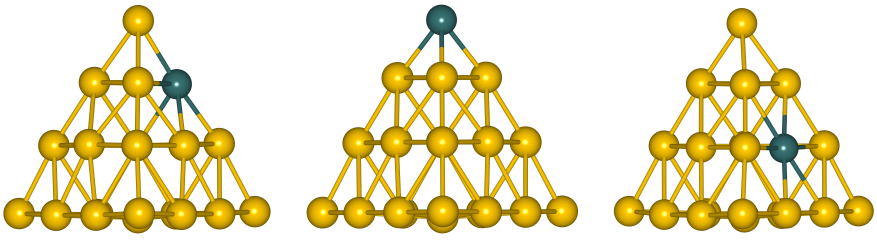

Figure 1: Most stable geometries of $Au_{19}Pt^-$ cluster. The values within the parenthesis indicate the relative energies of the corresponding structure w.r.t the most stable isomer Td-E.

geometry. The optimized geometries of the Td-V-V, Td-S-S and Td-E-E are shown in Figure 2. Interestingly, it is observed that the Td-V isomer becomes the most stable after adsorbing a CO_2 molecule.

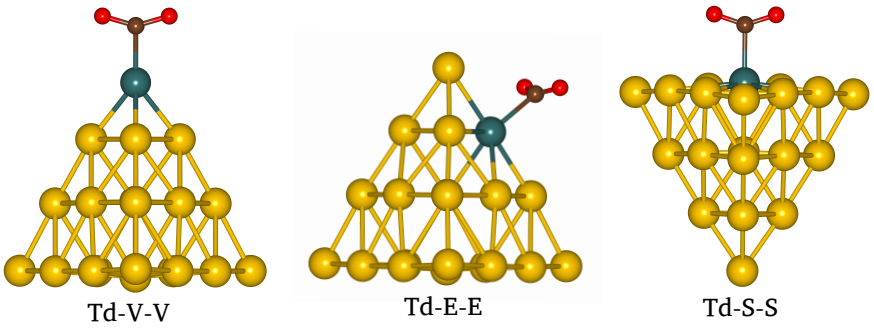

Figure 2: Most stable geometries of $Au_{19}Pt\text{-}CO_2^-$ cluster.

To quantify the strength of interaction between the cluster and CO_2 molecule we calculate the adsorption energy (E_{ads}) using the following equation,

$$E_{ads} = E(cluster - CO_2) - E(cluster) - E(CO_2) \tag{3}$$

where $E(cluster{-}CO_2)$, $E(cluster)$, $E(CO_2)$ are the energies of the cluster-CO_2 complex, anionic cluster on which CO_2 is adsorbed and a bare CO_2 molecule, respectively. The negative value of E_{ads} indicates the energetically favourable adsorption of CO_2 molecule on the clusters. More negative value of E_{ads} indicates stronger adsorption of CO_2 on the clusters. The results of E_a for all the isomers of $Au_{19}Pt^-$ are compiled in Table 1. Note

that we explore all the possible sites in $Au_{19}Pt^-$ cluster for the adsorption of CO_2, however, except Pt-site all other sites exhibit non-adsorbing behaviour for CO_2. We find that the vertex-Pt site is more favorable for the adsorption of CO_2 molecule. The corresponding CO_2 adsorption energy is found to be -0.34 eV, whereas, CO_2 adsorption energy for the case of surface-Pt site is obtained as -0.15 eV which is almost half of that observe for the case of vertex-Pt site. These values are small but significant as the capturing of highly stable CO_2 molecule is very challenging task. Here, it is important to highlight that our study finds that a CO_2 molecule does not get adsorbed on the pure anionic Au_{20} cluster.

Table 1: Adsorption energies (E_{ads}) of CO_2, bond length, bond angle of CO_2 and Bader charge on CO_2 on various sites of $Au_{19}Pt^-$ cluster along with distances (Pt-C and Pt-O) between CO_2 and Pt-atom obtained with RPBE XC functional and Grimme's D3 correction

	E_a(eV)	bond length (Å)			bond angle (∠OCO) (°)	Bader charge on CO_2 (e)
system		Pt-C	Pt-O	C-O		
gas-phase CO_2				1.18	180	
Td-V-V	-0.34	2.09	2.71	1.23	146	-0.42
Td-E-E	-0.24	2.17	2.78	1.22	146	-0.41
Td-S-S	-0.15	2.17	2.81	1.22	143	-0.43

For the hydrogenation reaction, the activation of CO_2 plays an important role which has been highlighted in our earlier work.[3] To analyze the activation of CO_2 on the $Au_{19}Pt^-$ we calculate the C-O bond lengths and O-C-O bond angle, which are listed in Table 1. From this table it is observed that for the adsorption of CO_2 on Pt-sites of $Au_{19}Pt^-$, both the C-O bond lengths are elongated by 0.04-0.05 Å as compared to those of the gas-phase CO_2 values. Moreover, the O-C-O bond angle is also changed from the gas-phase value of 180° to 143°-146° for the CO_2 adsorption on different Pt sites. These results indicate that the electronic structure of CO_2 gets disturbed when it is adsorbed on Pt-doped gold cluster.[53,54] This in turn indicates that we can activate CO_2 by adsorbing it on Pt site in $Au_{19}Pt^-$ cluster. The activation of CO_2 on $Au_{19}Pt^-$ cluster can be explained with the help of charge

transfer from the cluster to the CO_2 molecule. The charge distribution in the cluster has been calculated using Bader's charge analysis.[55] From last column of Table 1 we can see that for all the clusters the charge transfer takes place from cluster to CO_2 molecule.

The correlation between the activation of CO_2 and the charge on it, can also be observed from the charging of CO_2 molecule in the gas phase. In Table 2 we list different charging states of CO_2 molecule along with its bond lengths and bond angles. These results clearly show that the presence of charge on CO_2 even in the gas phase activates this molecule. It is observed that the charge is transfer to the anti-bonding orbital of CO_2, which leads to the activation of this molecule.[53,54]

Table 2: Different charge state of CO_2 in the gas phase and the corresponding bond length and angle obtained with RPBE XC functional and Grimme's D3 correction

Charge (e)	C-O-bond length (Å)	bond angle (∠OCO) (°)
0.00	1.18	180
-1.00	1.26	133
-2.00	1.34	114

To get more insight into the mechanism of activation of CO_2 molecule we compare the projected DOS (PDOS) of CO_2 adsorbed on Pt-sites in Td-V, Td-S and Td-E clusters with that of the free CO_2 molecule. The corresponding projected DOSs are shown in Figure 3. From this figure we observe that the p-orbitals of the O- and C-atoms are highly disturbed and get broadened. This indicates that the C=O bond in CO_2 gets activated when it is adsorbed on Pt site of the doped cluster, which is reflected in the bond lengths and bond angle data of CO_2 in Table 1. Moreover, from the Figure 3 it can be seen that the activated CO_2 molecule is adsorbed through the interaction mainly between the p-orbital of O-atom in CO_2 molecule and the d-orbital of Pt-atom in the clusters.

Nest, we analyze the reason for CO_2 molecule exhibiting different degree of adsorption when adsorbed on different sites of $Au_{19}Pt^-$ cluster. The adsorption energy depends on the degree of interaction between the CO_2 and the cluster. To understand the different degrees of interaction between CO_2 and the isomers of $Au_{19}Pt^-$ cluster we plot the PDOS of d-

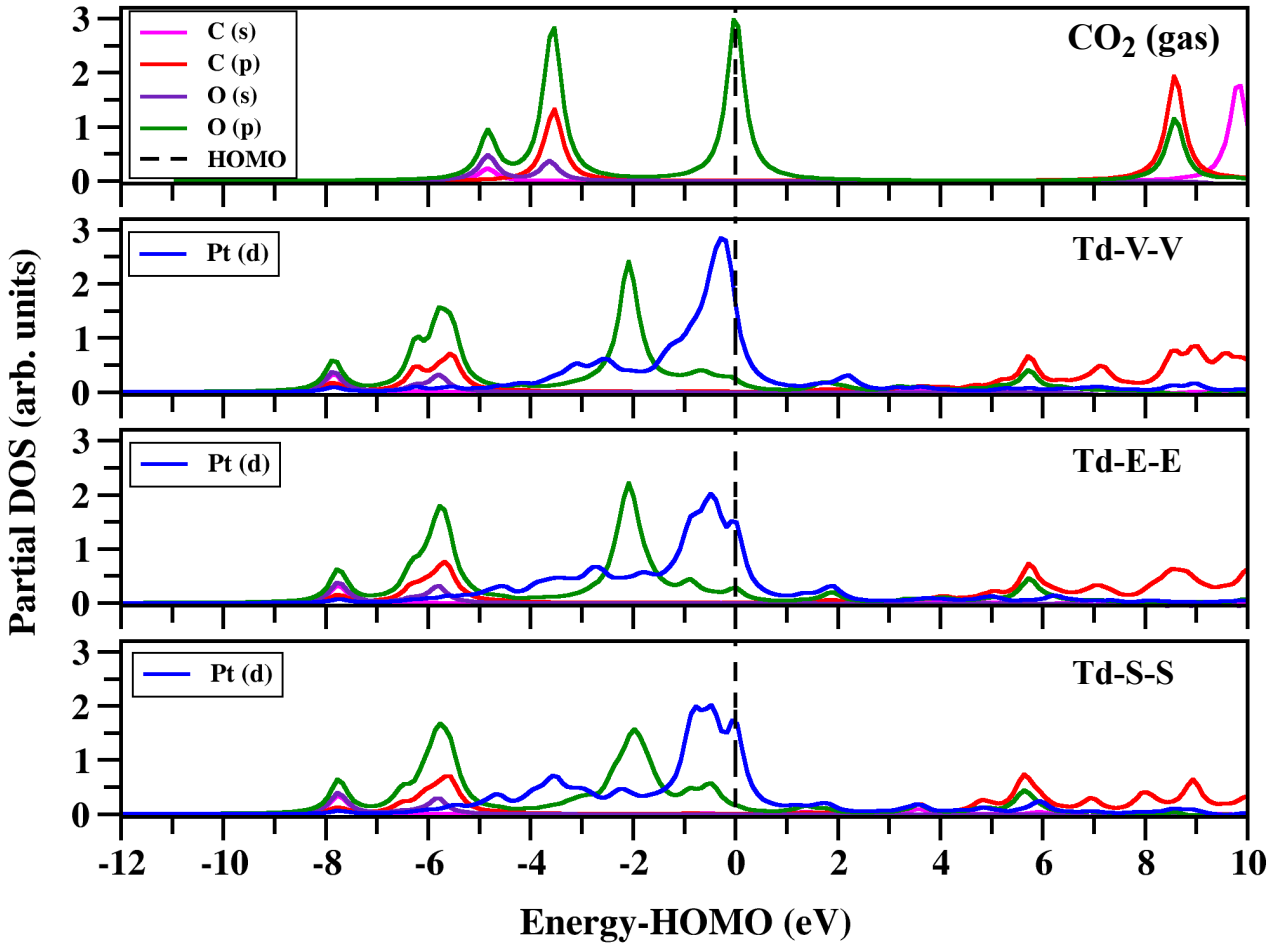

Figure 3: Partial-DOS of free CO_2 molecule (top pannel) and CO_2 molecule adsorbed on vertex-Pt of Td-V, edge-Pt of Td-E, and surface-Pt of Td-S cluster, respectively.

orbitals of vertex-, edge- and surface-Pt atoms in Figure 4. From this figure it can be seen that the availability of partially filled d-orbital near HOMO is more for the case of vertex-Pt atom as compared to that of the edge- and surface-Pt atoms. This is because of the low coordination of the vertex-Pt as compared to the edge- and surface-Pt atoms. Consequently, the cluster with vertex-Pt atom interacts with CO_2 molecule more strongly as compared to other isomers.

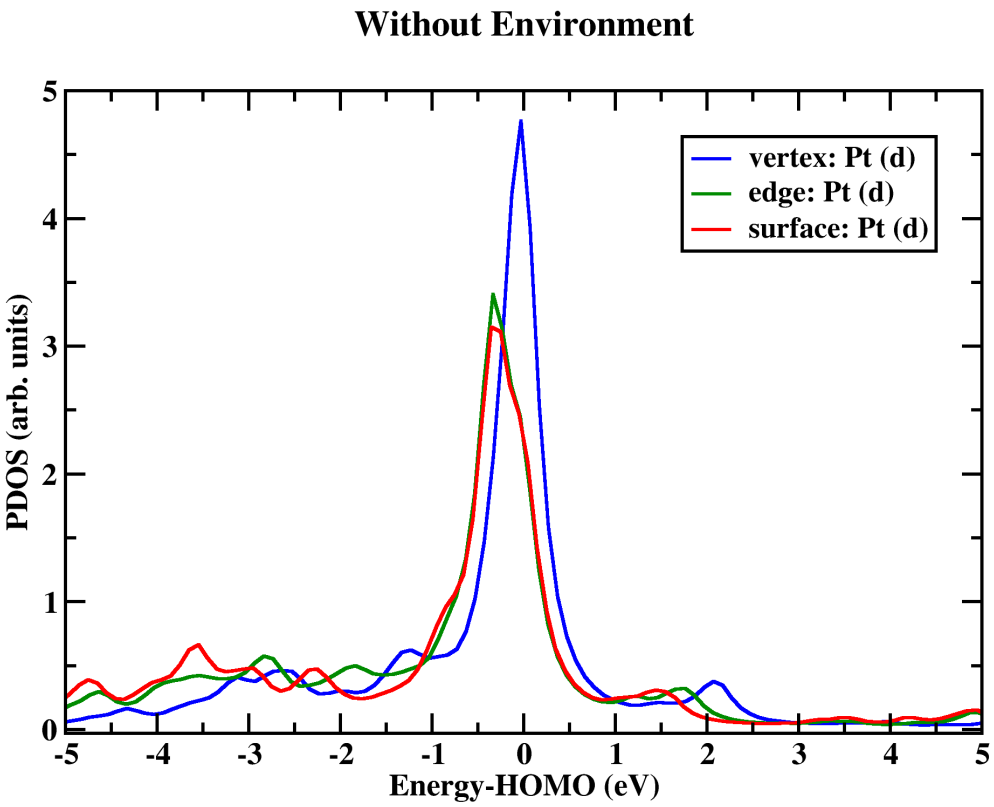

Figure 4: Partial-DOS of d-orbital of Pt-atom in different clusters.

Interaction of CO_2 with $Au_{19}Pt^-$ in Water

In this section we discuss the effect of water environment on the adsorption and activation of CO_2 molecule interacting with $Au_{19}Pt^-$ clusters. For this purpose we use implicit solvent model COSMO,[56] as implemented in ADF. In the water environment, the adsorption energy of CO_2 on the clusters has been calculated using the following equation:

$$E_a^{env} = E^{env}(cluster - CO_2) - E^{env}(cluster) - E^{env}(CO_2) \tag{4}$$

where $E^{env}(cluster - CO_2)$, $E^{env}(cluster)$, $E^{env}(CO_2)$ are the energies of the cluster-CO_2 complex, anionic cluster, and a CO_2 molecule submerged in aqueous medium, respectively.

In Table 3 we compile the data for the adsorption energy and C-O bond lengths of CO_2

Table 3: Adsorption energies (E_{ads} and E_{ads}^{env}) of CO_2 , C-O bond length (C-O), bond angle of CO_2 ($\angle$OCO) and Bader charge on CO_2 (q^b) on various sites of $Au_{19}Pt^-$ cluster with and without environment obtained with RPBE XC functional and Grimme's D3 correction

	without water environment			with water environment		
properties	Td-V-V	Td-E-E	Td-S-S	Td-V-V	Td-E-E	Td-S-S
adsorption energy (eV)	-0.34	-0.24	-0.15	-0.52	-0.45	-0.60
C-O (Å)	1.23	1.22	1.22	1.24	1.24	1.25
$\angle$OCO (°)	146	146	143	139	136	135
q^b (e)	-0.42	-0.41	-0.43	-0.62	-0.69	-0.68

when it gets adsorbed on $Au_{19}Pt^-$ in the water environment. For comparison, in this table we also tabulate the corresponding data for the case of without water. From Table 3 we observe that for the adsorption of CO_2 in aqueous medium, Td-S structure is slightly (0.06 eV) more reactive than Td-V, which was found to be the most reactive site in gas-phase. Moreover, Td-E is found to be slightly less reactive than both Td-S and Td-V. Now, in the following we highlight the interesting data in Table 3. From this table it can be seen that in the aqueous environment CO_2 is 0.18-0.45 eV more strongly bonded with the negative ions of $Au_{19}Pt$ as compared to that of the corresponding cases of without water. These results clearly indicate that the negative ions of $Au_{19}Pt$ can capture CO_2 more efficiently in aqueous medium. The strong interaction between the CO_2 molecule and the anions in water may be attributed to the enhanced electrostatic interaction due to the presence of the dielectric aqueous medium. To understand the activation of the adsorbed CO_2 on $Au_{19}Pt^-$ in the presence of water we calculate the C-O bond-lengths and $\angle$OCO which are listed in Table 3. For comparison we also list here the corresponding C-O bond-length and $\angle$OCO data for the cases of without aqueous environment. From Table 3 we can see that in aqueous environment the adsorbed CO_2 molecule gets more elongated (0.01 - 0.03 Å) and the $\angle$OCO is more displaced (7-12°) from the linear value of 180° as compared to the values for the corresponding cases of without water. These results indicate that the adsorbed CO_2 molecule in aqueous medium is more activated as compared to that of the gas phase cases. Such higher activation can be attributed to more charge transfer (last row of Table 3) from the cluster to CO_2 in the

presence of water. From our study it is clear that water acts as a promoter for the adsorption and activation of CO_2 on $Au_{19}Pt^-$ cluster.

Since the clusters are kept in the water environment the interaction of water molecules with the cluster is important for the CO_2 molecule to find open active sites within the clusters during the adsorption process. Therefore, we also investigate the interaction of a single water molecule with $Au_{19}Pt^-$ clusters and compare it with that between CO_2 and $Au_{19}Pt^-$ clusters. The corresponding data are compiled in Table 4.

Table 4: Adsorption of a single H_2O molecule on Pt-atom of $Au_{19}Pt^-$ cluster along with the adsorption energy, E_a for the corresponding cases of CO_2 with environment obtained with RPBE XC functional and Grimme's D3 correction

clusters	H_2O adsorption energy (eV)	CO_2 adsorption energy (eV)
Td-V	-0.22	-0.52
Td-E	-0.26	-0.45
Td-S	-0.32	-0.60

From this table we find that in aqueous medium a single water molecule gets adsorbed prefarably on the surface-Pt site of Td-S cluster and the corresponding adsorption energy is found to be -0.32 eV which is almost half of that observed for the adsorption of CO_2 on Td-S (-0.60 eV). This clearly indicates that in aqueous medium CO_2 molecule gets preferably adsorbed on Td-S over the adsorption of water molecule on this cluster. Similarly, for the cases of Td-V and Td-E the adsorption of CO_2 is much stronger than that of the water molecule. Therefore, it is clear that for all the anions of $Au_{19}Pt$ cluster the adsorption of CO_2 molecule will not be hindered by the water molecule in aqueous medium.

Conclusion

We investigate the adsorption and activation of CO_2 molecule on the anions of $Au_{19}Pt$ cluster using ab-initio density functional method. We show that the isomers of $Au_{19}Pt$ cluster are negatively charged even at zero potential in the water environment with Pt-cathode. In the

gas phase, it is observed that CO_2 molecule gets preferably adsorbed on the vertex-Pt site of the anions of $Au_{19}Pt$ clusters. We find that the adsorption of CO_2 molecule on Pt-doped gold clusters occurs through the hybridization between p-orbital of O-atom in CO_2 and the partially filled d-orbital of Pt atom of $Au_{19}Pt^-$ clusters. The adsorbed CO_2 gets activated due to the charge transfer from the cluster to the anti-bonding state of this molecule. In aqueous medium, both the surface- and vertex-Pt sites are found to be the most reactive for the adsorption of a CO_2 molecule. Moreover, the adsorption of CO_2 on anions of $Au_{19}Pt$ cluster dominates over that of water molecule in aqueous medium. Therefore, it is clear that the water molecules cannot hinder the interaction between the CO_2 and the cluster. Instead, it is observed that the water can enhance the adsorption and the activation of the adsorbed CO_2 molecule. In contrast, we observe that CO_2 molecule does not get adsorbed or activated on the anion of pure 20-atoms Au_{20} gold cluster. Therefore, it is very interesting to note that use of small amount of Pt atoms at suitable sites on gold cluster can lead to a novel compound for capturing the activated CO_2 molecule. Such compound may act as potential catalyst for the electrocatalytic hydrogenation of this activated CO_2 towards various complexes like methanol, OME, DME etc. which has the potential to be the source of energy in the future.

Acknowledgement

KM acknowledges the Department of Science and Technology, Government of India, for funding (DST/INSPIRE/04/2018/002482). The authors are thankful for the computing time provided on HBNI RRCAT-Supercomputer facilities. KM would like to acknowledge CINECA, Italy for providing supercomputing facilities.

Supporting Information Available

In the supporting information we provide the results corresponding to PBE with Grimme's D3 dispersion correction and the coordinates of the $Au_{19}Pt$-CO_2 complexes.

References

(1) Hansen, J.; Nazarenko, L.; Ruedy, R.; Sato, M.; Willis, J.; Del Genio, A.; Koch, D.; Lads, A. e.; Lo, K.; Menon, S.; Novakov, T.; Perlwitz, J.; Russ ell, G.; Schmidt, G. A.; Tausnev, N. Earth's Energy Imbalance: Confirmation and Implications. *Science* **2005**, *308*, 1431–1435.

(2) Michele, A.; Angela, D. *The Carbon Dioxide Revolution*; Springer International Publishing: Springer Nature Switzerland AG, 2021.

(3) Reichenbach, T.; Mondal, K.; Jäger, M.; Vent-Schmidt, T.; Himmel, D.; Dybbert, V.; Bruix, A.; Krossing, I.; Walter, M.; Moseler, M. Ab initio study of CO2 hydrogenation mechanisms on inverse ZnO/Cu catalysts. *Journal of Catalysis* **2018**, *360*, 168 – 174.

(4) Malte Behrens, Heterogeneous Catalysis of CO2 Conversion to Methanol on Copper Surfaces - Behrens - 2014 - Angewandte Chemie International Edition - Wiley Online Library. *Angew. Chem. Int. Ed.* **2014**, *53*, 12022–12024.

(5) Kattel, S.; Ramírez, P. J.; Chen, J. G.; Rodriguez, J. A.; Liu, P. Active sites for CO2 hydrogenation to methanol on Cu/ZnO catalysts. *Science* **2017**, *355*, 1296–1299.

(6) Zheng, W.; Nayak, S.; Yuan, W.; Zeng, Z.; Hong, X.; A. Vincent, K.; Edman Tsang, S. C. A tunable metal–polyaniline interface for efficient carbon dioxide electro-reduction to formic acid and methanol in aqueous solution. *Chem. Comm. 52*, 13901–13904.

(7) Weiran, Zheng,; Wing,Man Ho ,; Lin,Ye ,; Edman,Tsang Shik Chi, Electroreduction of Carbon Dioxide to Formic Acid and Methanol over a Palladium/Polyaniline Catalyst in Acidic Solution: A Study of the Palladium Size Effect. *Energy Technology 5*, 937–944.

(8) Shanmugam, R.; Thamaraichelvan, A.; Kuppusamy Ganesan, T.; Viswanathan, B. Carbon dioxide activation and transformation to HCOOH on metal clusters (M = Ni, Pd, Pt, Cu, Ag & Au) anchored on a polyaniline conducting polymer surface – an evaluation study by hybrid density functional theory. *RSC Advances 6*, 100829–100840.

(9) Ma, J.; Sun, N.; Zhang, X.; Zhao, N.; Xiao, F.; Wei, W.; Sun, Y. *Catal. Today* **2009**, *148*, 221.

(10) Liu, X. M.; Lu, G. Q.; Yan, Z. F.; Beltramini, J. *Ind. Eng. Chem. Res.* **2003**, *42*, 6518.

(11) Song, C. *Catal. Today* **2006**, *115*, 2.

(12) Lee, S. *Methanol Synthesis Technology*; CRC Press, 1989.

(13) Behrens, M.; Studt, F.; Kasatkin, I.; Kühl, S.; Hävecker, M.; Abild-Pedersen, F.; Zander, S.; Girgsdies, F.; Kurr, P.; Kniep, B.-L.; Tovar, M.; Fischer, R. W.; Nørskov, J. K.; Schlögl, R. The Active Site of Methanol Synthesis over Cu/ZnO/Al2O3 Industrial Catalysts. *Science* **2012**, *336*, 893–897.

(14) Lunkenbein, T.; Schumann, J.; Behrens, M.; Schlögl, R.; Willinger, M. G. Formation of a ZnO Overlayer in Industrial Cu/ZnO/Al2O3 Catalysts Induced by Strong Metal–Support Interactions. *Angew. Chem. Int. Ed.* **2015**, *54*, 4544–4548.

(15) Graciani, J.; Mudiyanselage, K.; Xu, F.; Baber, A. E.; Evans, J.; Senanayake, S. D.; Stacchiola, D. J.; Liu, P.; Hrbek, J.; Sanz, J. F.; Rodriguez, J. A. Highly active copper-ceria and copper-ceria-titania catalysts for methanol synthesis from CO2. *Science* **2014**, *345*, 546–550.

(16) Sahu, A.; Mondal, K.; Ghosh, P. Microscopic understanding of electrocatalytic reduction of CO2 on Pd-polyaniline composite: an ab initio study. *Journal of Molecular Modeling* **2018**, *24*, 248.

(17) Zheng, W.; Nayak, S.; Yuan, W.; Zeng, Z.; Hong, X.; Vincent, K. A.; Tsang, S. C. E. A tunable metal–polyaniline interface for efficient carbon dioxide electro-reduction to formic acid and methanol in aqueous solution. *Chem. Commun.* **2016**, *52*, 13901–13904.

(18) Nitopi, S.; Bertheussen, E.; Scott, S. B.; Liu, X.; Engstfeld, A. K.; Horch, S.; Seger, B.; Stephens, I. E. L.; Chan, K.; Hahn, C.; Norskov, J. K.; Jaramillo, T. F.; Chorkendorff, I. Progress and Perspectives of Electrochemical CO_2 Reduction on Copper in Aqueous Electrolyte. *Chemical Reviews* **2019**, *119*, 7610–7672.

(19) Lv, W.; Zhou, J.; Kong, F.; Fang, H.; Wang, W. Porous tin-based film deposited on copper foil for electrochemical reduction of carbon dioxide to formate. *International Journal of Hydrogen Energy* **2016**, *41*, 1585–1591.

(20) Li, S.; Alfonso, D.; Nagarajan, A. V.; House, S. D.; Yang, J. C.; Kauffman, D. R.; Mpourmpakis, G.; Jin, R. Monopalladium Substitution in Gold Nanoclusters Enhances CO2 Electroreduction Activity and Selectivity. *ACS Catalysis* **2020**, *10*, 12011–12016.

(21) Mistry, H.; Reske, R.; Zeng, Z.; Zhao, Z.-J.; Greeley, J.; Strasser, P.; Cuenya, B. R. Exceptional Size-Dependent Activity Enhancement in the Electroreduction of CO2 over Au Nanoparticles. *J. Am. Chem. Soc.* **2014**, *136*, 16473–16476, PMID: 25325519.

(22) Ismail, A. M.; Samu, G. F.; Balog, A.; Csapo/, E.; Jana/ky, C. Composition-Dependent Electrocatalytic Behavior of Au–Sn Bimetallic Nanoparticles in Carbon Dioxide Reduction. *ACS Energy Letters* **2019**, *4*, 48–53.

(23) Vickers, J. W.; Alfonso, D.; Kauffman, D. R. Electrochemical Carbon Dioxide Reduction at Nanostructured Gold, Copper, and Alloy Materials. *Energy Technology* **2017**, *5*, 775–795.

(24) Chadha, G.; Chug, P. Enhanced CO2 adsorption on doped Au32 gold nanocages: A density functional approach. *Materials Research Express* **2018**, *5*, 065038.

(25) Rong, H.; Ji, S.; Zhang, J.; Wang, D.; Li, Y. Synthetic strategies of supported atomic clusters for heterogeneous catalysis. *Nature Communications* **2020**, *11*, 5884.

(26) Choi, H.; Oh, S.; Park, J. Y. High methane selective Pt cluster catalyst supported on Ga2O3 for CO2 hydrogenation. *Catalysis Today* **2020**, *352*, 212–219, Special Issue for the 17th Korea-Japan Symposium on Catalysis.

(27) Yang, C.-T.; Wood, B. C.; Bhethanabotla, V. R.; Joseph, B. The effect of the morphology of supported subnanometer Pt clusters on the first and key step of CO2 photoreduction. *Phys. Chem. Chem. Phys.* **2015**, *17*, 25379–25392.

(28) Sun, Y.; Cai, X.; Hu, W.; Liu, X.; Zhu, Y. Electrocatalytic and photocatalytic applications of atomically precise gold-based nanoclusters. *Science China Chemistry* **2020**,

(29) Lu, Y.; Zhang, C.; Li, X.; Frojd, A. R.; Xing, W.; Clayborne, A. Z.; Chen, W. Significantly enhanced electrocatalytic activity of Au25 clusters by single platinum atom doping. *Nano Energy* **2018**, *50*, 316–322.

(30) Mondal, K.; Banerjee, A.; Ghanty, T. K. Structural and Chemical Properties of Subnanometer-Sized Bimetallic $Au_{19}Pt$ Cluster. *J. Phys. Chem. C* **2014**, *118*, 11935–11945.

(31) Mondal, K.; Banerjee, A.; Fortunelli, A.; Ghanty, T. K. Does enhanced oxygen activation always facilitate CO oxidation on gold clusters? *Journal of Computational Chemistry* **2015**, *36*, 2177–2187.

(32) te Velde, G.; Bickelhaupt, F. M.; Baerends, E. J.; Fonseca Guerra, C.; van Gisbergen, S. J. A.; Snijders, J. G.; Ziegler, T. Chemistry with ADF. *J. Comput. Chem.* **2001**, *22*, 931–967.

(33) Baerends, E. J. et al. ADF2017, SCM, Theoretical Chemistry, Vrije Universiteit, Amsterdam, The Netherlands, https://www.scm.com.

(34) van Lenthe, E.; Baerends, E. J.; Snijders, J. G. Relativistic total energy using regular approximations. *The Journal of Chemical Physics* **1994**, *101*, 9783–9792.

(35) Perdew, J. P.; Burke, K.; Ernzerhof, M. Generalized gradient approximation made simple. *Phys. Rev. Lett.* **1996**, *77*, 3865–3868.

(36) Beletskaya, A. V.; Pichugina, D. A.; Shestakov, A. F.; Kuz'menko, N. E. Formation of H2O2 on Au20 and Au19Pd Clusters: Understanding the Structure Effect on the Atomic Level. *The Journal of Physical Chemistry A* **2013**, *117*, 6817–6826, PMID: 23859501.

(37) Jiang, D.-e.; Whetten, R. L. Magnetic doping of a thiolated-gold superatom: First-principles density functional theory calculations. *Phys. Rev. B* **2009**, *80*, 115402.

(38) Ma, W.; Chen, F. CO oxidation on the Ag-doped Au nanoparticles. *Catalysis letters* **2013**, *143*, 84–92.

(39) Zhang, X. D.; Guo, M. L. Electronic structure and optical transitions of Au20- xCux nanoclusters. *Journal of nanoscience and nanotechnology* **2010**, *10*, 7192–7195.

(40) BROYDEN, C. G. The Convergence of a Class of Double-rank Minimization Algorithms: 2. The New Algorithm. *IMA Journal of Applied Mathematics* **1970**, *6*, 222–231.

(41) Fletcher, R. A new approach to variable metric algorithms. *The Computer Journal* **1970**, *13*, 317–322.

(42) Goldfarb, D. A family of variable-metric methods derived by variational means. *Mathematics of computation* **1970**, *24*, 23–26.

(43) Shanno, D. F. Conditioning of quasi-Newton methods for function minimization. *Mathematics of computation* **1970**, *24*, 647–656.

(44) Momma, K.; Izumi, F. VESTA 3 for three-dimensional visualization of crystal, volumetric and morphology data. *J. Appl. Crystallogr.* **2011**, *44*, 1272–1276.

(45) Hammer, B.; Hansen, L. B.; Nørskov, J. K. Improved adsorption energetics within density-functional theory using revised Perdew-Burke-Ernzerhof functionals. *Phys. Rev. B* **1999**, *59*, 7413–7421.

(46) Hensley, A. J. R.; Ghale, K.; Rieg, C.; Dang, T.; Anderst, E.; Studt, F.; Campbell, C. T.; McEwen, J.-S.; Xu, Y. DFT-Based Method for More Accurate Adsorption Energies: An Adaptive Sum of Energies from RPBE and vdW Density Functionals. *The Journal of Physical Chemistry C* **2017**, *121*, 4937–4945.

(47) Grimme, S.; Antony, J.; Ehrlich, S.; Krieg, H. A consistent and accurate ab initio parametrization of density functional dispersion correction (DFT-D) for the 94 elements H-Pu. *The Journal of Chemical Physics* **2010**, *132*, 154104.

(48) Forster-Tonigold, K.; Groß, A. Dispersion corrected RPBE studies of liquid water. *The Journal of Chemical Physics* **2014**, *141*, 064501.

(49) Chang, L.; Cheng, D.; Sementa, L.; Fortunelli, A. Hydrogen evolution reaction (HER) on Au@Ag ultrananoclusters as electro-catalysts. *Nanoscale* **2018**, *10*, 17730–17737.

(50) Kibler, L. A. Hydrogen Electrocatalysis. *ChemPhysChem* **2006**, *7*, 985–991.

(51) Langenbach, E.; Spitzer, A.; Lüth, H. The adsorption of water on Pt(111) studied by irreflection and UV-photoemission spectroscopy. *Surface Science* **1984**, *147*, 179 – 190.

(52) Jain, S. C.; Krishnan, K. S. The thermionic constants of metals and semi-conductors I. Graphite. *Proceedings of the Royal Society of London. Series A. Mathematical and Physical Sciences* **1952**, *213*, 143–157.

(53) M, A. *Carbon Dioxide Recovery and Utilization*; Springer Netherlands: Springer Science+Business Media Dordrecht, 2003.

(54) Cheng, D.; Negreiros, F. R.; Aprà, E.; Fortunelli, A. Computational Approaches to the Chemical Conversion of Carbon Dioxide. *ChemSusChem* **2013**, *6*, 944–965.

(55) Richard. F. W., B. *Atoms in Molecules: A Quantum Theory*; Oxford University Press: Oxford University Press, New York, 1990.

(56) Klamt, A.; Schüürmann, G. COSMO: a new approach to dielectric screening in solvents with explicit expressions for the screening energy and its gradient. *J. Chem. Soc., Perkin Trans. 2* **1993**, 799–805.

Graphical TOC Entry